

# Heterodimer Magnetic Nanoparticles-Carbon Nanotubes with Tunable Magnetic Properties

Leandro N. Monsalve<sup>1</sup>, Laura Pampillo<sup>2</sup>, Ricardo Martinez<sup>3</sup>, and Mariano Escobar<sup>1,\*</sup>

<sup>1</sup>INTI - CONICET, Av. Gral. Paz 5445 San Martín (1650), Buenos Aires, B1650, Argentina

<sup>2</sup>Instituto de Tecnología y Ciencias de la Ingeniería “Ing. Hilario Fernández Long”, UBA-CONICET, Facultad de Ingeniería, Ciudad Autónoma de Buenos Aires, C1063ACV, Argentina

<sup>3</sup>Universidad Nacional de Formosa – CONICET, Campus Universitario, Modulo I, Av. Gutnisky 3200, Formosa, Argentina

This work proposes an easy and scalable convergent synthesis method to obtain heterodimers formed by multi-walled carbon nanotubes and magnetic nanoparticles via carbon-nitrogen bonds. Magnetic nanoparticles were synthesized by solvothermal method. Heterodimers were characterized by X-ray diffraction, Fourier Transform Infrared Spectroscopy, Transmission Electronic Microscopy and magnetic properties. The magnetic nanoparticles have a mixed crystal structure, mostly formed by maghemite and a small fraction of hematite. Infrared Spectroscopy and Transmission Electronic Microscopy confirm the formation of heterodimer magnetic nanoparticles—carbon nanotubes via covalent bonds. Magnetic measurement indicates that it is possible to adjust the magnetic response according to the final application.

**Keywords:** Heterodimer, Magnetic Nanocomposite, Carbon Nanotube, Maghemite.

## 1. INTRODUCTION

The study of iron oxide nanoparticles has been of great interest in technology and fundamental science due to their unique electrical and magnetic properties.<sup>1</sup> The finite size and surface effects in nano-dimensions of iron oxides impact on the magnetic, electrical and optical properties relative to the bulk, which cause to be aroused remarkable phenomena such as super-paramagnetism.<sup>2,3</sup> These super-paramagnetic properties have promising applications in data storage, nuclear magnetic resonance imaging and sensors.<sup>4,5</sup> The three main forms of iron oxide are magnetite (Fe<sub>3</sub>O<sub>4</sub>), maghemite (γ-Fe<sub>2</sub>O<sub>3</sub>) and hematite (α-Fe<sub>2</sub>O<sub>3</sub>).

Due to their high surface area and unique mechanical and electrical properties, carbon nanotubes (CNT) have been proposed for a wide range of applications: composite materials,<sup>6–8</sup> separation,<sup>9</sup> electronic devices,<sup>10,11</sup> drug delivery<sup>12,13</sup> and so forth. They are commercially available and their production at multigram scale is well developed.

Several methods have been developed for the functionalization of CNTs.<sup>14</sup> These methods were useful for the attachment of small organic moieties, polymers, nanoparticles and biomolecules to the surface of CNTs. Among

these methods, air oxidation of carbon nanotubes is easy to perform and environmentally friendly. Compared to acid oxidation (HNO<sub>3</sub>:H<sub>2</sub>SO<sub>4</sub> 1:3) air oxidation does not produce acid waste and introduces less sidewall defects.<sup>15</sup>

The preparation of magnetic CNTs can be achieved by the decoration of carbon nanotubes with iron oxide nanoparticles. These composites have promising applications for cell tracking and imaging,<sup>16</sup> selective targeting of tumors for drug delivery,<sup>17,18</sup> signal enhancement for immuno-electrochemical sensors.<sup>19,20</sup> The study of the physico-chemical properties of these nanostructures is important in order to determine their viability for these applications.

According to the literature, there are two ways to obtain magnetic nanocomposites: (i) synthesis of magnetic nanoparticles *in situ* or, (ii) convergent synthesis (the nanostructures comprising the heterodimer are synthesized separately and combined in the last step of synthesis).

As example of the former strategy, Kozhuharova et al. have filled multi-walled carbon nanotubes (MWCNT) on silicon substrate viable pyrolysis of ferrocene/cobaltocene mixtures.<sup>21</sup> Moreover, CNTs can be chemically modified in order to provide them additional functionalities. As example of the second strategy, iron oxide nanoparticles can be attached to CNTs either by covalent bonding or

\*Author to whom correspondence should be addressed.

electrostatic attraction. CNTs are usually oxidized to create negatively charged carboxylate groups that binds positively charged iron oxide nanoparticles or acts as nucleation site for nanoparticle growth.<sup>22–24</sup> Covalent bonding of iron oxide nanoparticles to CNTs yields more stable composites with better processability.

Tuning the magnetic properties of composite such as coercivity and magnetization saturation is highly desirable. Zhao et al.<sup>25</sup> have synthesized magnetic Fe/CNTs composite with controllable Fe nanoparticle concentration. They have tested magnetic properties through hysteresis curves at 50 and 300 K, exhibiting a ferromagnetic behavior, which differs from the iron filled CNTs displaying superparamagnetic properties.<sup>26</sup> Moreover, their curves show clear saturation and the saturation magnetization (Ms) is about 125 emu/g-Fe, which is much lower than that of the bulk iron (218 emu/g-Fe). Dillon et al.<sup>27</sup> have tuned the magnetic properties of iron-filled multi-wall carbon nanotubes synthesized by the pyrolysis of ferrocene in a two zone furnace. Magnetic characterization of the Fe/CNTs revealed that their coercivity can be systematically tuned by varying the pyrolysis temperature, whereas the saturation magnetization can be significantly enhanced by optimization of the sublimation temperature. Sun et al. have fabricated magnetic carbon nanotube by employing a one-step approach, in which ferrocene decomposed at high temperatures of 350 °C, 425 °C, 500 °C, and transformed into iron oxides to deposit on CNTs. Magnetic measurements demonstrated that the composites prepared at 500 °C were ferromagnetic, while the composites obtained at 350 °C and 425 °C became superparamagnetic and showed no remanence or coercivity.<sup>26</sup>

In this paper, we propose a facile synthesis method to obtain heterodimers formed by multi-walled carbon nanotubes and magnetic nanoparticles via carbon-nitrogen bonds. Heterodimers were characterized by X-ray diffraction, Fourier Transform Infrared Spectroscopy, Transmission Electronic Microscopy and magnetic properties. It is interesting to note that it is possible to adjust the magnetic response according to the final application. These results are in agreement with previously reported data,<sup>25,26</sup> which synthesized magnetic carbon nanotubes and changed the magnetic behavior of the composite according to its composition. Compared to these reports, our method has the advantage of applying a convergent and scalable synthetic strategy from commercial carbon nanotubes. Moreover, iron oxide nanoparticle functionalization and coupling reaction could be performed at room temperature. Compared with other reports, our method has the advantage of applying a convergent and scalable synthetic strategy from commercial carbon nanotubes.

## 2. EXPERIMENTAL DETAILS

Multiwalled carbon nanotubes (from Nanocyl 7000),  $\text{Fe}(\text{NO}_3)_3 \cdot 9\text{H}_2\text{O}$ , ethylene glycol, isopropanol,

2-aminopropyl-triethoxysilane (APTS), thionyl chloride, methylene chloride, pyridine were used straight from the bottle.

The magnetic nanoparticles (NP) were prepared as follow: 2 g of  $\text{Fe}(\text{NO}_3)_3 \cdot 9\text{H}_2\text{O}$  were dissolved in 10 ml of  $\text{H}_2\text{O}$  and 10 ml of ethylene glycol. The solution was heated up to 100 °C on a hot plate and evaporated to give a gel and then was kept warm until complete evaporation of solvent. The material that was not stuck to the bottom of the beaker was collected and heated at 300 °C for 3 hours in inert atmosphere, cooled to room temperature in the oven and stored.

Heterodimers Magnetic NP-CNT were prepared according to the procedure depicted in Figure 1.

Carbon nanotubes were oxidized for 8 hours in a muffle furnace at 400 °C. After that, 50 mg of oxidized CNT were weighed in a clean, dry round-bottom flask. Then 6 ml of thionyl chloride were added, the flask was firmly capped and the reaction was sonicated at 80 °C for one hour and a half. After this, the product was filtered, obtaining Chloride-CNT (Cl-CNT). The black precipitate was washed with methylene chloride to remove thionyl chloride excess. Cl-CNT was used immediately in the subsequent reaction.

By other way, the surface of magnetic nanoparticles was functionalized with amino groups. The procedure was as follow: 50 mg of magnetic NP were weighed in a conical centrifuge tube and dispersed in 3 ml of isopropanol with ultrasound. Then 3 ml of amino propyl-triethoxysilane (APTS) were added and sonication was continued for 1 hour. Afterwards the suspension was centrifuged at 5000 rpm for 5 minutes and the supernatant was discarded. The pellet was washed with isopropanol, dispersed and centrifuged twice. The washed pellet was dried in vacuum oven at 60 °C for 24 h to obtain magnetic NP-NH<sub>2</sub>.

In order to form the heterodimer, the following procedure was used. NP-NH<sub>2</sub> was suspended in 5 ml of methylene chloride and was dispersed using ultrasound in a 125 ml Erlenmeyer with stopper. Once NP-NH<sub>2</sub> was dispersed 1 ml of pyridine was added. Sonication was maintained and then Cl-CNT was quickly added and the Erlenmeyer was quickly capped. After a few minutes the formation of conjugates was verified by the loss of red color of the suspension. Two hours later the suspension was filtered and the precipitate washed with methylene chloride. The precipitate was dried in vacuum oven at 60 °C for 24 h to obtain the heterodimers (HD) Magnetic NP-CNT. The heterodimers are designated according to the mass ratio between the nanoparticles and nanotubes. For instance, HD10 refers to the sample that contain 10 wt.% of magnetic nanoparticles respect to the mass of carbon nanotubes. They were prepared HD5, HD10, HD50, HD75 and HD100. The later has the same weight content of Magnetic NP and CNT.

Fourier transforms IR (FTIR) measurements were performed on a Shimadzu FTIR-8300 spectrophotometer in

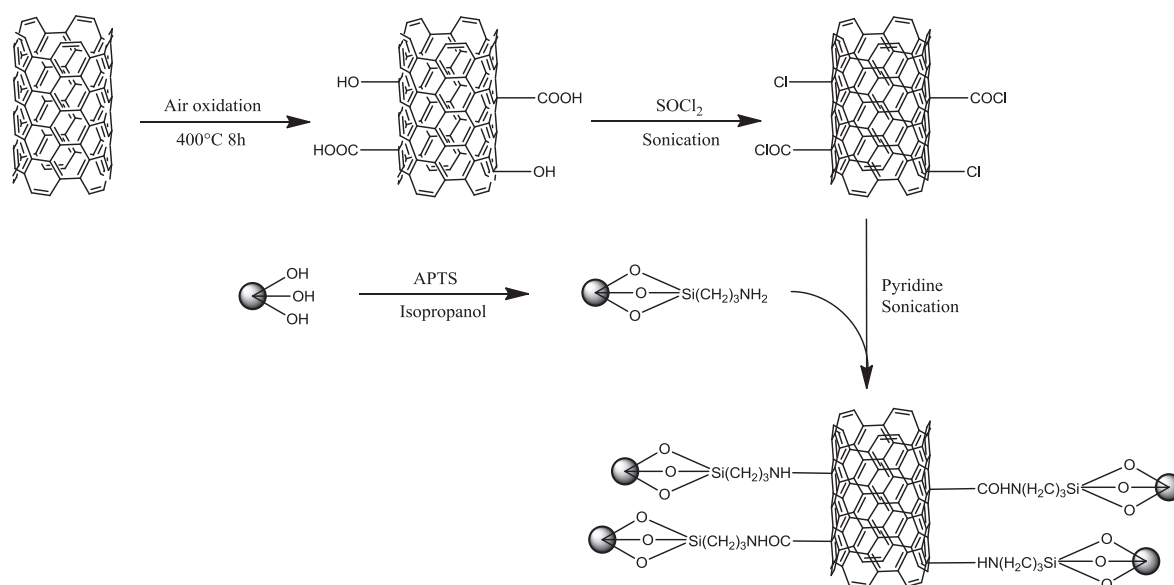


**Figure 1.** Reaction steps for the preparation of heterodimers magnetic NP-CNT.

film with KBr windows and an attenuated total reflectance (ATR) cell. Structural properties of powders were analyzed by X-ray diffraction (XRD) in a theta–2theta Rigaku diffractometer equipped with a vertical goniometer. Measurements were realized between  $20^\circ$  and  $80^\circ$  using  $\text{Cu-K}\alpha$  radiation. The magnetization versus applied magnetic field was measured with a Physical Property Measurement System (PPMS, Quantum Design) at 300 K up to 2 T. Morphology of the heterodimers was characterized by transmission Electronic Microscope (TEM-EM Philips 301).

### 3. RESULTS AND DISCUSSION

The composition of magnetic nanoparticles and heterodimers was analyzed by XRD (Fig. 2). The deconvolution of spectra indicates that nanoparticles are composed by a combination of oxides: a 90% of the sample corresponds to maghemite ( $\gamma\text{-Fe}_2\text{O}_3$ ) and 10% to hematite ( $\alpha\text{-Fe}_2\text{O}_3$ ). The former is ferrimagnetic and provides the

major contribution to the magnetism of the nanoparticles; the latter has weak antiferromagnetism and thus virtually all its magnetic moments are canceled.

The synthesis above described for obtaining magnetic nanoparticles leads to quasi-amorphous maghemite with some size distribution. Phase transformation of magnetite to hematite occurs when thermal energy is sufficient to induce diffusion of iron ions occupying tetrahedral sites to octahedral sites present in the compact stacking of the oxygen ions of the oxide. The heat treatment performed ( $300^\circ\text{C}$ ) in order to induce the growth of nanoparticles allows phase transformation. Usually, this process occurs around  $700^\circ\text{C}$  at micro scale, but  $300^\circ\text{C}$  is sufficient for this transformation to take place to a small extent. This explains the appearance of hematite as a minority phase.

The difference of particle size between the two phases is evidenced by different peak widths. Reflections corresponding to maghemite show wide peaks associated with small particle size. This widening indicates a crystalline

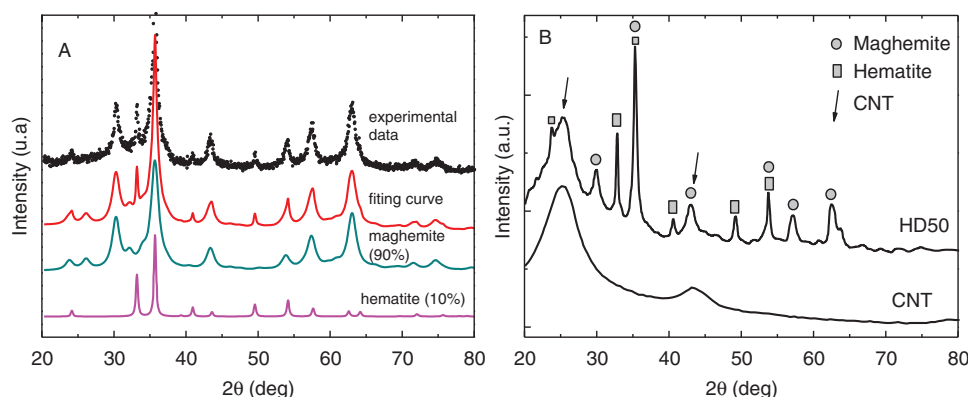


**Figure 2.** X-ray diffraction spectrum of (A) magnetic NP with deconvolution results, and (B) NTC and HD-50.



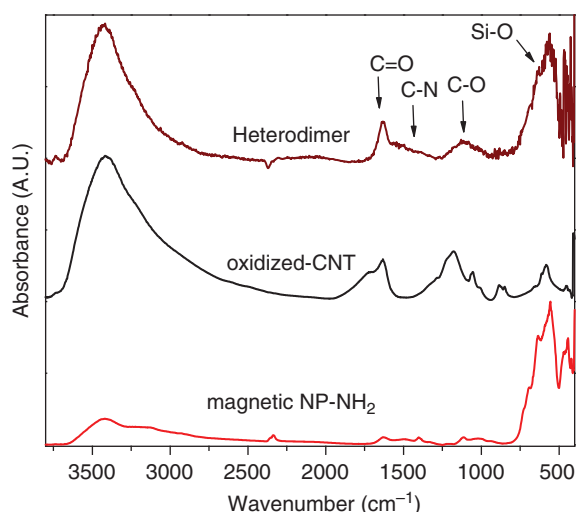


**Figure 3.** FTIR spectra of oxidized CNTs, magnetic NP treated with APTS and heterodimers. Characteristic bands of different moieties are indicated with arrows.

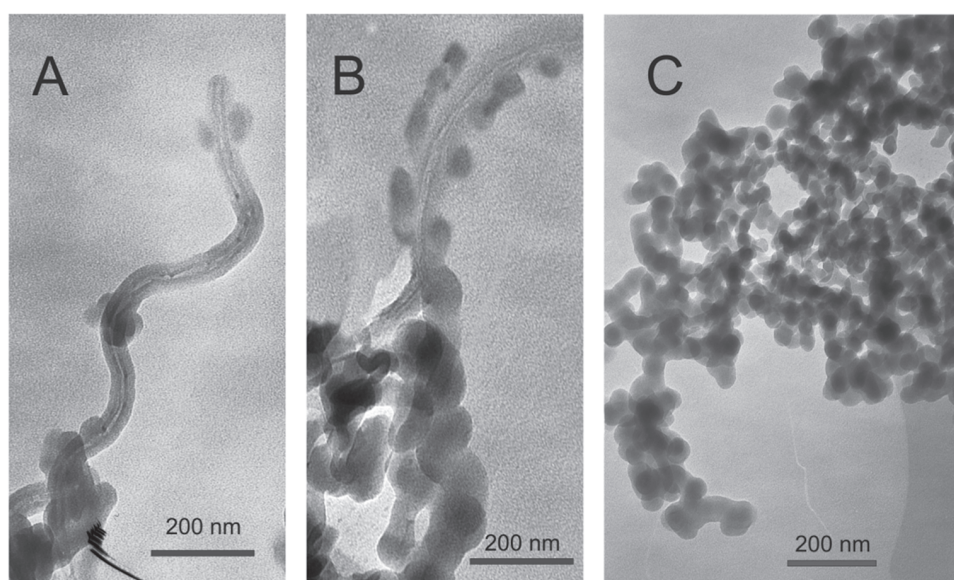
disorder, which has a significant effect on the magnetic properties of the material. Hematite has a crystallite size greater because it is more compact (no vacancies) and less energy is required for the process of nucleation and growth phase to occur. The pattern fitting of X-ray diffraction spectra allowed determining a crystallite size of 10 nm for maghemite and 40 nm for hematite.

FTIR spectra allow us to follow the different steps during the synthesis of heterodimers (Fig. 3). Magnetic NP treated with APTS showed strong absorption at  $556\text{ cm}^{-1}$  and  $633\text{ cm}^{-1}$  due to the deformations of  $\gamma\text{-Fe}_2\text{O}_3$  in the tetrahedral and octahedral sites. Absorptions due to Si-O-Si deformations were located at  $1019\text{ cm}^{-1}$  and  $1114\text{ cm}^{-1}$  which indicate the presence of silicon from

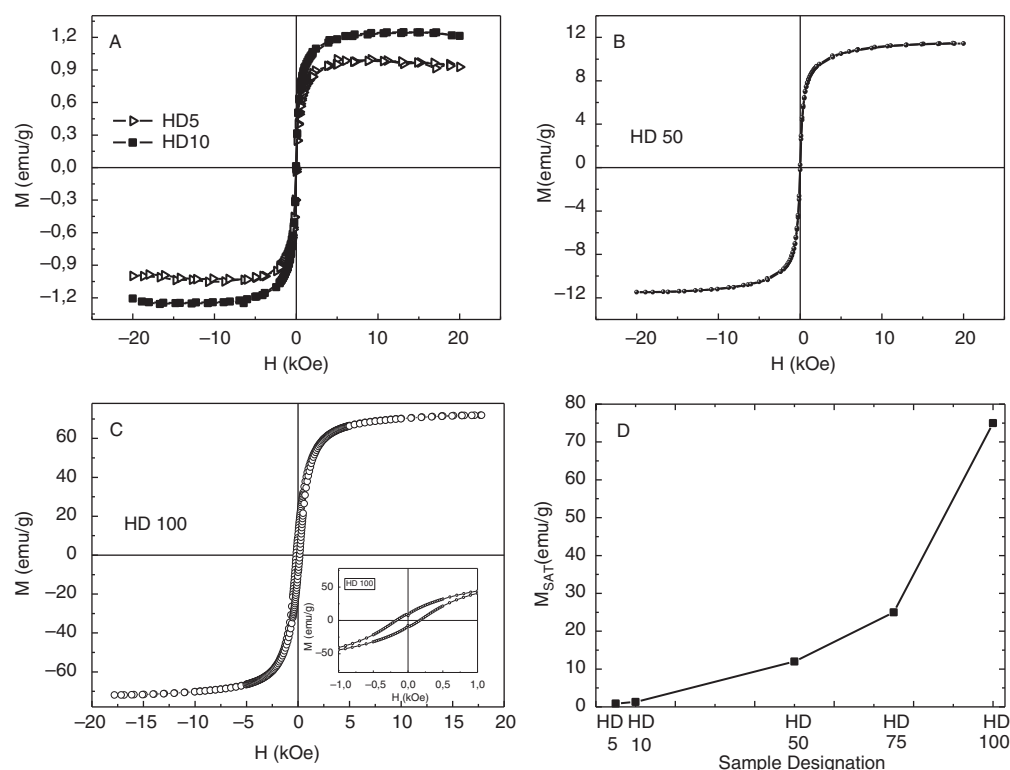
APTS. The presence of amino propyl moieties on the magnetic NP surface could be confirmed by the presence of absorptions at  $2913\text{ cm}^{-1}$  (C-H stretch),  $3243\text{ cm}^{-1}$  and  $3419\text{ cm}^{-1}$  (N-H stretch of primary amine).<sup>28</sup> Oxidized carbon nanotubes showed typical absorptions from oxygen moieties:  $1178\text{ cm}^{-1}$  (C-O stretch), a shoulder at  $1714\text{ cm}^{-1}$  (C=O stretch) and a broad band centered at  $3418\text{ cm}^{-1}$  (O-H stretch). The oxidized surface of carbon nanotubes consists of a mixture of oxygenated moieties including alcohol and carboxylic acid.<sup>29</sup> Spectrum of heterodimers showed bands from Fe-O deformations along with bands from oxygen moieties that remained unreacted. Absorption in the region of  $1400\text{--}1600\text{ cm}^{-1}$  was also present and can be attributed to the amide I, II and III, and C-N stretch from amine bands.<sup>30</sup> Amide I band could not be distinguished from the band at  $1633\text{ cm}^{-1}$  which was also present in pristine carbon nanotubes. The latter signals confirm the covalent attachment of maghemite nanoparticles onto carbon nanotubes. Moreover, the moieties present in heterodimers Magnetic NP-CNT in Figure 1 were fully identified by FTIR.

Figure 4 shows the TEM images of heterodimers with different Magnetic NP-CNT ratio. As observed, a rough coating layer consisting of numerous magnetic NP is homogeneously deposited onto the surface of MWCNT as the content of nanoparticles increase. As higher is the concentration of the nanoparticles, higher is the proportion of MWCNT's covered.

The magnetic characterization of the nanocomposites was made through M-H curves. Figure 5(A) presents the magnetic behavior of HD 5 and HD 10, which presents a super-paramagnetic behavior, with a saturation value near  $1\text{ emu/g}$ . Figure 5(B) shows the magnetic behavior of the HD 50, which also presents the superparamagnetic



**Figure 4.** TEM images of (A) HD 10, (B) HD 50 and (C) HD 100.



**Figure 5.** Magnetization versus applied field of: (A) HD 5 y HD10, (B) HD 50, (C) HD 100, (D) saturation magnetization as function of magnetic particles fraction.

character with a saturation value of about 12 emu/g. M–H curve for HD 100 is presented in Figure 5(C); the inset therein corresponds to the area near the origin, which exhibits a slight ferromagnetic character with non-zero remnant magnetization and coercivity. The saturation magnetization reaches a value of 73 emu/g. This system has a saturation value six times higher than that of HD 50. Figure 5(D) presents the saturation magnetization as function of magnetic nanoparticles fraction.

It is interesting to note that it is possible to adjust the magnetic response according to the final application. These results are in agreement with previously reported data,<sup>25,26</sup> which synthesized magnetic carbon nanotubes and changed the magnetic behavior of the composite according to its composition. Compared to these reports, our method has the advantage of applying a convergent and scalable synthetic strategy from commercial carbon nanotubes. Moreover, iron oxide nanoparticle functionalization and coupling reaction could be performed at room temperature.

#### 4. CONCLUSION

A facile and scalable synthesis of multiwalled carbon nanotubes decorated with covalently bonded magnetic nanoparticles at various concentrations (heterodimers Magnetic NP-CNT) via carbon-nitrogen bonds was proposed. The synthesized nanoparticles were mainly

magnetite and a little fraction of hematite. The surface modification of both, nanoparticles and carbon nanotubes, promotes covalent bond formation at room temperature. Both saturation magnetization and coercivity of the heterodimer could be tuned with the magnetic NP content. It was demonstrated that it is possible to adjust the magnetic response according to the final application. Compared with other reports, our method has the advantage of applying a convergent and scalable synthetic strategy from commercial carbon nanotubes.

**Acknowledgments:** We are grateful to INTI and ANPCyT (PICT 0423-2013) for partial financial support. LNM, RM and ME are staff of CONICET.

#### References and Notes

1. A. E. Panasencko, I. Tkachenko, L. Zemnukhova, I. Shchetinin, and N. Didenko, *J. Magn. Magn. Mater.* 405, 66 (2016).
2. K. Witte, W. Bodnar, T. Mix, N. Schell, G. Fulda, T. G. Woodcock, and E. Burkel, *J. Magn. Magn. Mater.* 403, 103 (2016).
3. S. Li, T. Zhang, R. Tang, H. Qiu, C. Wang, and Z. Zhou, *J. Magn. Magn. Mater.* 379, 226 (2015).
4. M. Arvand and M. Hassannezhad, *Materials Science and Engineering. C, Materials for Biological Applications* 36, 160 (2014).
5. H. Wu, G. Liu, Y. Zhuang, D. Wu, H. Zhang, H. Yang, and S. Yang, *Biomaterials* 32, 4867 (2011).
6. J. E. Kirk, I. Kinloch, A. Windle, J. K. Sandler, and M. S. Shaffer, *Polymer* 44, 5893 (2003).

7. P. Pötschke, B. Krause, S. T. Buschhorn, U. Köpke, M. Müller, T. Villmow, and K. Schulte, *Compos. Sci. Technol.* 74, 78 (2013).
8. D. Zilli, S. Goyanes, M. M. Escobar, C. Chilotte, V. Bekkeris, A. L. Cukierman, and G. Rubiolo, *Polym. Compos.* 64, 612 (2007).
9. L. Zhou, L. Ji, P. C. Ma, Y. Shao, H. Zhang, W. Gao, and Y. Li, *J. Hazard. Mater.* 265, 104 (2014).
10. Z. Xiao and F. E. Camino, *Nanotechnology* 20, 135205 (2009).
11. Y. Wu, X. Lv, B. Kang, and H. Wang, *International Conference on Optoelectronics and Microelectronics (ICOM)*, IEEE (2013), pp. 91–93, doi:10.1109/ICoOM.2013.6626498.
12. A. Masotti and A. Caporali, *International Journal of Molecular Sciences* 14, 24619 (2013).
13. S. Shao, L. Li, G. Yang, J. Li, C. Luo, T. Gong, and S. Zhou, *Int. J. Pharm.* 421, 310 (2011).
14. D. Tasis, N. Tagmatarchis, V. Georgakilas, and M. Prato, *Chemistry, an European Journal* 9, 4000 (2003).
15. P. Hou, C. Liu, and H. Cheng, *Carbon* 46, 2003 (2008).
16. E. Kılıç, *J. Magn. Magn. Mater.* 401, 949 (2016).
17. A. Faraj, A. Shaik, and B. A. Sayed, *Nanomedicine* 10, 931 (2015).
18. H. Wu, G. Liu, X. Wang, J. Zhang, Y. Chen, J. Shi, H. Yang, and H. Hu, *Acta Biomaterialia* 7, 3496 (2011).
19. F. Li, J. Han, L. Jiang, Y. Wang, Y. Li, Y. Dong, and Q. Wei, *Biosens. Bioelectron.* 68, 626 (2015).
20. D. Quesada and A. Merkoçi, *Biosens. Bioelectron.* 73, 47 (2015).
21. R. Kozhuharova, M. Ritschel, D. Elefant, A. Graff, I. Monch, T. Muhl, C. M. Schneider, and A. Leonhardt, *J. Magn. Magn. Mater.* 290, 250 (2005).
22. E. G. Uc-Cayetano, F. Avilés, J. V. Cauich-Rodríguez, R. Schönfelder, A. Bachmatiuk, M. Rummeli, and G. Cruz, *J. Nanopart. Res.* 16, 2192 (2014).
23. P. Xu, D. Cui, B. Pan, F. Gao, R. He, Q. Li, T. Huang, C. Bao, and H. Yang, *Appl. Surf. Sci.* 254, 5236 (2008).
24. W. Li, C. Gao, H. Qian, J. Ren, and D. Yan, *Journal of Material Chemistry* 16, 1852 (2006).
25. F. Zhao, H. Duan, W. Wang, and J. Wang, *Physica B* 407, 2495 (2012).
26. Z. Sun, Z. Liu, Y. Wang, B. Han, J. Du, and J. Zhang, *Journal of Material Chemistry* 15, 4497 (2005).
27. F. C. Dillon, A. Bajpai, A. Koo's, S. Downes, Z. Aslam, and N. Grobert, *Carbon* 50, 3674 (2012).
28. C. Lu, H. Bai, B. Wu, F. Su, and J. Hwang, *Energy Fuels* 22, 3050 (2008).
29. M. Escobar, S. Goyanes, M. Corcuera, A. Eceiza, I. Mondragon, G. Rubiolo, and R. Candal, *J. Nanosci. Nanotechnol.* 9, 6228 (2009).
30. M. Ghazanfari and A. Yazdani, *Mater. Sci. Semicond. Process.* 40, 152 (2015).

Received: 10 March 2016. Accepted: 29 June 2016.

IP: 5.101.219.67 On: Thu, 05 Apr 2018 11:56:53  
Copyright: American Scientific Publishers  
Delivered by Ingenta